

Facile synthesis of *N*-benzylanilines via the amination of toluene over a cobalt-based catalyst

Fei-Feng Mao, Wen-Qiang Gong, Song Han, Yan Zhou, Ming-Shuai Sun*, Zhang-Min Li, Duan-Jian Tao*

National Engineering Research Center for Carbohydrate Synthesis, Key Laboratory of Fluorine and Silicon for Energy Materials and Chemistry of Ministry of Education, College of Chemistry and Chemical Engineering, Jiangxi Normal University, Nanchang 330022 China

ARTICLE INFO

Keywords:

Oxidative amination
N-benzylanilines
 Carbon material
 Cobalt-based catalyst

ABSTRACT

Utilizing aromatic alkanes instead of aromatic oxygenated compounds as the starting materials for efficient synthesis of *N*-benzylanilines remains a great challenge, which is hampered because of the chemical inertia property of aromatic alkanes. Herein, a cost-effective and promising cascade protocol was proposed for synthesis of *N*-benzylanilines via the amination of toluene over a cobalt-based catalyst. Both the intermediate benzaldehyde and target product *N*-benzylanilines could be achieved in 99 % yield with the optimized conditions. Moreover, comparative experiments and characterization further clarified that the cascade synthesis of *N*-benzylaniline was through the amination of toluene involving oxidation, condensation, and hydrogenation reactions. Metallic cobalt loaded on Co-N-C/800-0.1 accounted for such superior catalytic performance. Furthermore, the Co-N-C/800-0.1 catalyst also showed good applicability and reusability. This study offers a potential avenue for direct synthesis of aromatic amines from available and inexpensive aromatic alkanes.

1. Introduction

Aromatic alkanes are plentiful in fossil resources, and they serve as starting materials for numerous chemical intermediates and products [1]. They are commonly used as solvents or fuels, but their applications in organic synthesis are limited by their chemical inertia [2–4]. Significant progress in the functionalization of aromatic alkanes over the past few decades has enabled the conversion of low-value aromatic alkanes to obtain various aromatic oxygenated compounds such as aromatic ketones, alcohols, and acids [5–9]. The acquirement of aromatic oxygenated compounds from aromatic alkanes relies on many methods such as carbene insertion, C–H bond activation, and free-radical-mediated substitution/addition catalyzed by various transition metals [10–13].

Compared with aromatic oxygenated compounds, aromatic amines show higher added value and more functions in dyes, surfactants, pesticides, explosives, additives and so on [14,15]. Aromatic oxygenated compounds reacting with nitrogen-containing compounds are a common route for synthesizing aromatic amines. For example, Ma and his co-workers synthesized the Co nanoparticles loaded on the nitrogen-doped carbon for the synthesis of *N*-benzylanilines via the

N-alkylation of benzylic primary alcohols and anilines [16]. Xu and his co-workers also used a nickel-based catalyst for preparing *N*-benzylanilines by reductive amination of benzyl aldehydes [17]. Although *N*-benzylanilines could be readily synthesized with benzylic alcohols or benzyl aldehydes as raw materials (Scheme 1, Route A), these aromatic oxygenated compounds are mainly derived from the oxidation of aromatic alkanes. The synthesis of *N*-benzylanilines via the Route A has to require an additional oxidation reaction of aromatic alkane.

Recently, some studies directly used toluene instead of benzaldehyde or benzyl alcohol as raw material to synthesize *N*-benzylanilines over various homogeneous or heterogeneous catalysts (Scheme 1, Route B). However, this route still suffers from many drawbacks such as the requirements of noble metals, organic oxidants (e.g., DTBP, TBHP), or strong bases (e.g., KOtBu) and poor catalyst recyclability [18–22]. So far, N-containing porous carbon materials loaded with Co nanoparticles (Co-N-C) possess large specific surface area as well as rich mesopores, etc. [23–26]. As well known, N atoms as dopant into carbon can improve the activity of catalytic oxidation and condensation reactions [27], and Co nanoparticles also play a role in activating H₂ molecules [28,29]. Thereby, it is highly anticipated to design a N–C supported Co nanoparticles catalyst for efficient cascade synthesis of *N*-benzylanilines via

* Corresponding authors.

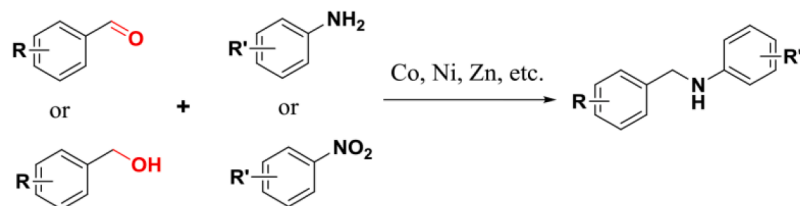
E-mail addresses: mingshuaisun@jxnu.edu.cn (M.-S. Sun), djtao@jxnu.edu.cn (D.-J. Tao).

<https://doi.org/10.1016/j.mcat.2024.113912>

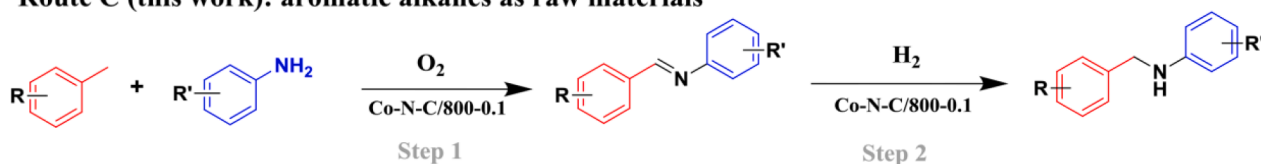
Received 22 November 2023; Received in revised form 31 January 2024; Accepted 1 February 2024

Available online 6 February 2024

2468-8231/© 2024 Elsevier B.V. All rights reserved.

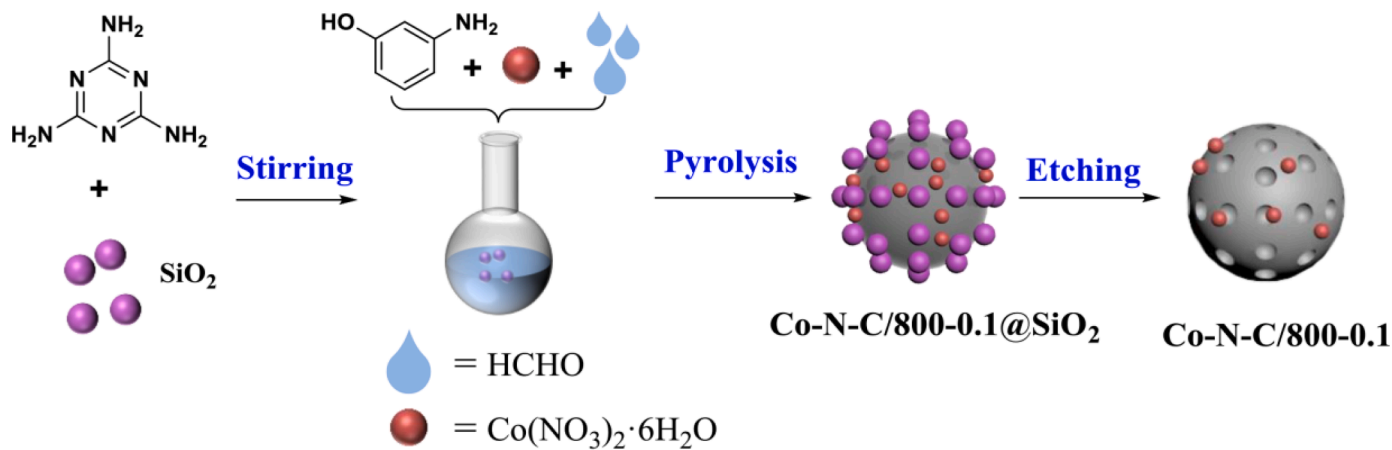
Route A: aromatic oxygenated compounds as raw materials**Route B: aromatic alkanes as raw materials**

☒ Noble metals ☒ Organic oxidants ☒ Strong bases ☒ Poor catalyst recyclability

Route C (this work): aromatic alkanes as raw materials

☑ High selectivity ☑ High yield ☑ No base or any additive ☑ Non-noble metals ☑ Excellent reusability

Scheme 1. Various routes for the synthesis of *N*-benzylanilines.



Scheme 2. Schematic illustration for the preparation of Co-N-C/800-0.1 catalyst.

the amination of toluene involving oxidation, condensation, and hydrogenation reactions (Scheme 1, Route C).

Herein, a set of heterogeneous Co-N-C catalysts were designed and fabricated using colloidal silica as hard template together with high temperature pyrolysis and subsequent acid etching. Moreover, their catalytic performance in cascade synthesis of *N*-benzylanilines was studied in detail. Various characterizations techniques and controlled experimental study were also performed to clarify the paths of those reactions. Finally, the applicability and stability of the prepared catalyst were further tested.

2. Experimental section

2.1. Materials

Colloidal silica (30 wt%) was purchased from Sigma Aldrich Co., Ltd. 3-Aminophenol (98 %), aniline (99 %), melamine (99 %), cobalt (II) nitrate hexahydrate (99 %), and formaldehyde (37 wt% in water) were commercially acquired from Shanghai Macklin Biochemical Co., Ltd. Toluene (99 %), 3-chlorotoluene (99 %), 4-chloroaniline (99 %), 2-phenylethylamine (99 %), 4-bromoaniline (99 %), *p*-anisidine (99 %), 3, 5-dimethylaniline (99 %), *p*-toluidine (99 %), *p*-fluorotoluene (98 %), and 4-fluoroaniline (99 %) were purchased from Adamas-Beta Co., Ltd. All chemicals were received and used without additional purification.

2.2. Catalyst preparation

As shown in Scheme 2, colloidal silica (5.0 g) and melamine (1.0 g) were dispersed in deionized water (50 mL). The dispersion was stirred at room temperature for 30 min. Subsequently, 3-aminophenol (0.5 g) and 10 mL of cobalt (II) nitrate solution (0.1 M) were simultaneously added to the mixture and dispersed by stirring for another 30 min. Subsequently, 0.75 mL of formaldehyde solution was added dropwise into the slurry and stirred vigorously for 24 h. The precipitate was gained by centrifugation and flushed with water. After that, the precipitate was treated by drying in a vacuum oven at 70 °C for 6 h to get the catalyst precursor. The precursor was loaded in a tubular furnace, heated to 800 °C at a heating rate of 3 °C/min, and kept for 2 h under protection of N₂ (25 mL/min). The black powder obtained after cooling in the furnace was named as Co-N-C/800-0.1@SiO₂. Finally, the Co-N-C/800-0.1@SiO₂ was treated with a 10 wt% hydrofluoric acid solution for 6 h followed by washing with water until pH≈7.0. The powder was dried overnight in the vacuum oven at 80 °C, which labeled Co-N-C/800-0.1.

For comparison, the reference catalysts Co-N-C/700-0.1 and Co-N-C/900-0.1 were prepared with similar procedure of Co-N-C/800-0.1 in which 700 and 900 represented the calcination temperature (°C). Then, the preparation procedure Co-N-C/800-0.2 was similar to that of Co-N-C/800-0.1, except for the different added amounts of Co(NO₃)₂·6H₂O (10 mL, 0.2 M). The catalyst prepared by the same steps as Co-N-C/800-0.1 without the adding nitrogen source was named as Co-C catalyst. In addition, the nitrogen-doped carbon material named as NC catalyst was prepared without using Co(NO₃)₂·6H₂O as raw material.

2.3. Characterization of Co-N-C catalysts

The N₂ adsorption/desorption analysis was carried out on a TriStar II 3020 device (Micromeritics). XRD analysis was conducted using a Rigaku RINT-2200 X-ray diffractometer with a Cu K α radiation. The scan range was from 5° to 90°, and the scan speed was 20°/min. Surface elements and their valence states were obtained by X-ray photoelectron spectroscopy (XPS) on an AXIS Supra of Kratos Analytical using Al K α as radiation source ($h\nu = 1486.7$ eV). The binding energies were calibrated based on the C 1s peak at 284.8 eV. The catalyst morphology was determined by a JEOL JEM-2100 transmission electron microscopy (TEM) instrument and a HITACHI SU8020 scanning electron microscope (SEM) instrument. The cobalt content in the sample was determined by inductively coupled plasma optical emission spectrometry (ICP-OES) employing an Agilent 720 ICP-OES device.

2.4. Catalytic performance

The cascade synthesis of *N*-benzylaniline was carried out under continuous stirring in a 25 mL stainless-steel autoclave. In a typical run, aniline (0.5 mmol), the catalyst (20 mg), and toluene (3 mL) were placed in the autoclave. Afterwards, the air inside was exchanged with oxygen several times and the O₂ pressure was maintained at 0.4 MPa before reaction. Subsequently, the reaction was performed with a stirring rate of 600 rpm at 160 °C for 12 h. Then the first reaction finished, the reactor cooled down to room temperature. Subsequently, pure H₂ was purged into the autoclave several times to replace the O₂ and maintained at 0.8 MPa before reaction. Then, the second step of the cascade synthesis was performed at 150 °C for 12 h. The liquid product was separated by filtration and analyzed using a Thermo Trace 1310 GC instrument equipped with an FID and a TG-5HT capillary column (30 m × 0.25 mm × 0.25 μ m). The molecular structures of products were identified by gas chromatography–mass spectrometry (GC–MS) on the Thermo Trace 1300 GC-ISQ instrument.

Co-N-C/800-0.1 was recycled through the procedure including centrifugation, washing with ethanol, and drying in the vacuum oven (70 °C, 8 h). Then, the recycled Co-N-C/800-0.1 was directly used in the subsequent cycle of *N*-benzylanilines synthesis.

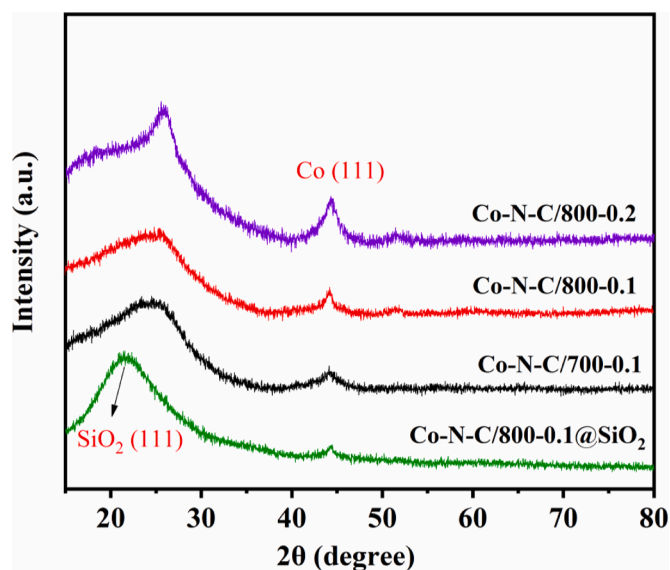


Fig. 1. XRD patterns of Co-N-C/700-0.1, Co-N-C/800-0.1, Co-N-C/800-0.2, and Co-N-C/800-0.1@SiO₂ catalysts.

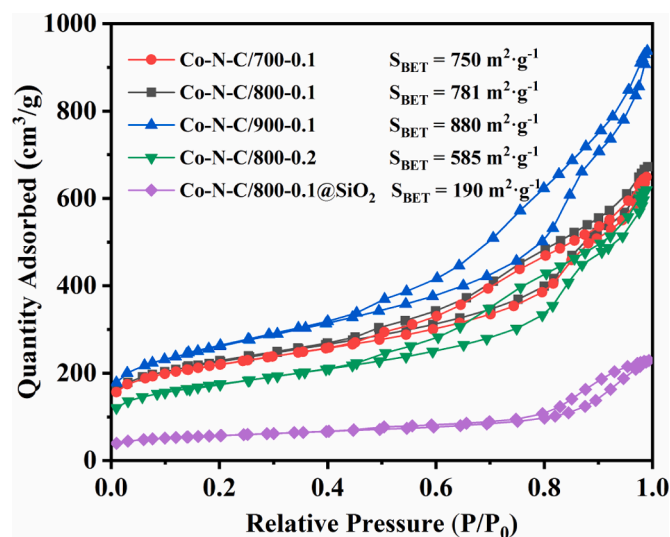


Fig. 2. N₂ adsorption–desorption isotherms of Co-N-C/700-0.1, Co-N-C/800-0.1, Co-N-C/900-0.1, Co-N-C/800-0.2, and Co-N-C/800-0.1@SiO₂ catalysts.

3. Results and discussion

3.1. Catalyst characterization

The phase structures of Co-N-C catalysts were studied by XRD analysis and the results are shown in Fig. 1. The diffraction peaks at $2\theta = 26^\circ$ belonged to the (002) lattice planes of graphitic carbon with certain defects and Co, N dopants [30,31]. Meanwhile, the diffraction peak at $2\theta = 22^\circ$ for Co-N-C/800-0.1@SiO₂ was attributed to the (111) crystal plane of silica [32]. Notably, another diffraction peaks at $2\theta = 44.2^\circ$ were assigned to the (111) lattice planes of the Co phase (PDF#15-0806) [33]. It is found that the increasing calcination temperature and Co loading would strengthen the peak intensity of metallic Co⁰. Comparing the XRD profiles of Co-N-C/800-0.1@SiO₂ and Co-N-C/800-0.1, the removal of SiO₂ also resulted in a significant enhancement of Co diffraction peak intensity. In addition, the XRD patterns of several reference catalysts NC, Co-C, and Co-N-C/900-0.1 were also displayed in Figure S1.

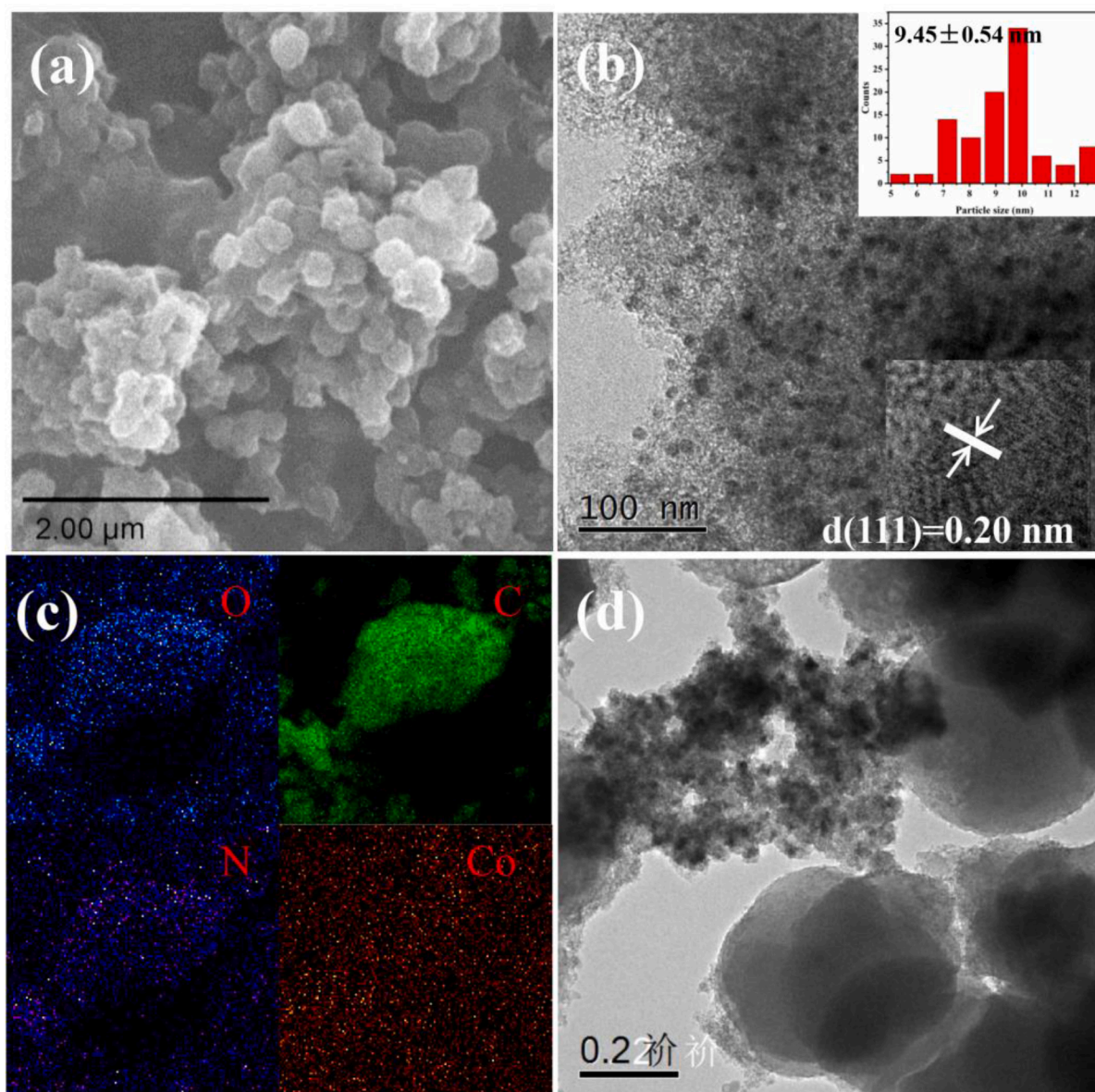


Fig. 3. (a) SEM image of the Co-N-C/800-0.1. (b) TEM (inset: Co nanoparticle size distribution and HRTEM) image of Co-N-C/800-0.1; and (c) corresponding elemental mappings of the Co-N-C/800-0.1. (d) TEM image of the Co-N-C/900-0.1.

The N_2 adsorption–desorption curves of as-prepared catalysts at $-196\text{ }^\circ\text{C}$ were tested as shown in Fig. 2. These isotherms all exhibited the typical characteristic of the type IV isotherm with a H3 hysteresis loop (Fig. 2) [34–36], showing the existence of the mesoporous structure [37]. Except for the Co-N-C/800-0.1@SiO₂ catalyst, each of the above catalysts adsorbed a significant amount of N_2 at the beginning of the adsorption process (Fig. 2). When the relative pressure ranged from 0.50 to 0.95, the amounts of N_2 adsorbed by the catalysts increased rapidly, indicating the catalysts possessing slit-shaped pores [38]. The pore size distribution curves were depicted in Figure S2, revealed that most of the pores in the catalysts were 10–20 nm in diameter, confirming that the catalysts are mesoporous materials. The specific surface area of Co-N-C/900-0.1, Co-N-C/800-0.1 and Co-N-C/700-0.1 catalysts was calculated to be 880, 781, and 750 $\text{m}^2\text{ g}^{-1}$, respectively, indicating that increasing annealing temperature would enlarge the catalyst's specific surface area. In addition, the specific surface area of Co-N-C/800-0.2 was 585 $\text{m}^2\text{ g}^{-1}$ while the Co-N-C/800-0.1 was 781 $\text{m}^2\text{ g}^{-1}$, indicating excessive metal loading would reduce the specific surface area. Moreover, Co-N-C/800-0.1@SiO₂ had the specific surface area of 190 $\text{m}^2\text{ g}^{-1}$,

which is significantly lower than the case of Co-N-C/800-0.1 (781 $\text{m}^2\text{ g}^{-1}$). It implies that the removal of silica could notably increase the specific surface area of Co-N-C catalysts. Larger specific surface area can provide much more available reactive sites, which has a positive effect in catalytic activity [39,40]. According to the results of ICP-OES (Table S1), Co-N-C/800-0.1@SiO₂ had a higher Co content than Co-N-C/800-0.1 catalyst, suggesting some cobalt species could be eliminated during the removal of silica by acid treatment [41].

To gain more morphology information, SEM and TEM characterizations were performed (Fig. 3). The SEM image of Co-N-C/800-0.1 (Fig. 3a) showed its spherical-like structure. And the TEM image (Fig. 3b) depicted that the Co nanoparticles were highly dispersed on the nitrogen-doped carbon support materials with an average size of 9.45 ± 0.54 nm. However, according to Scherrer's formula, the average Co crystallite size of Co-N-C/800-0.1 was calculated to 11.6 nm. It is worth noting that the calculated Co crystallite size differs from the TEM image result, potentially attributed to the inherent measurement error in XRD for small particles. Moreover, the high-resolution TEM image (the inset in Fig. 3b) exhibited lattice fringes with an intercrystalline spacing of

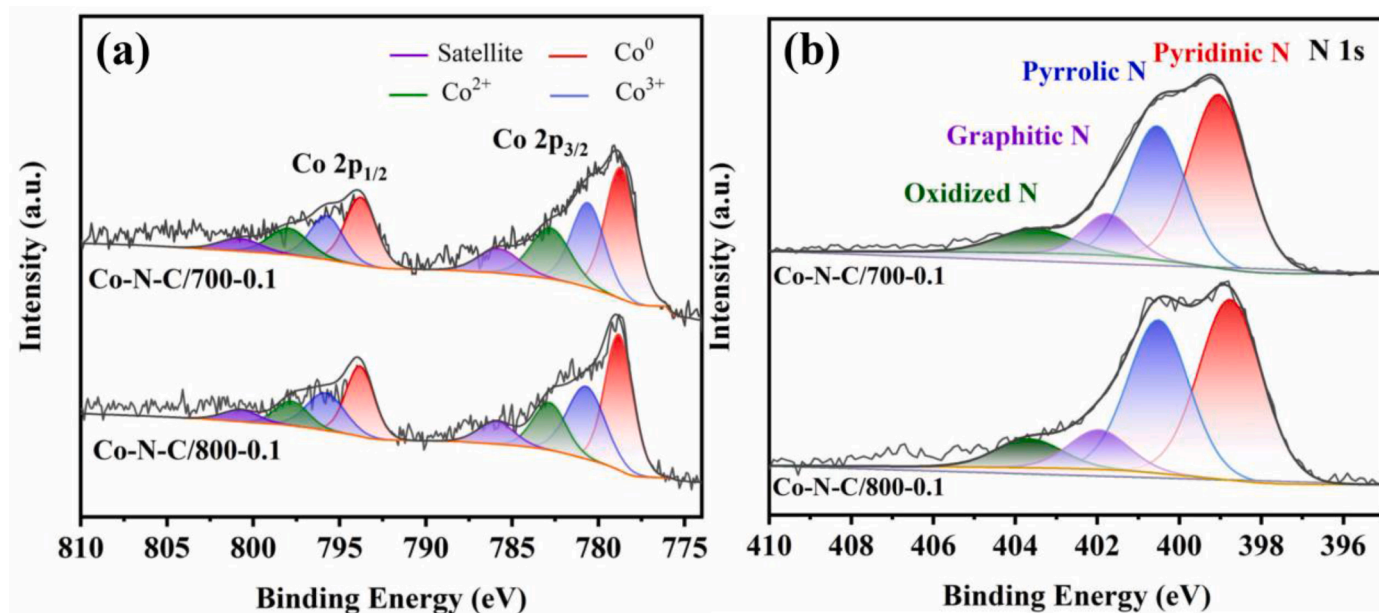
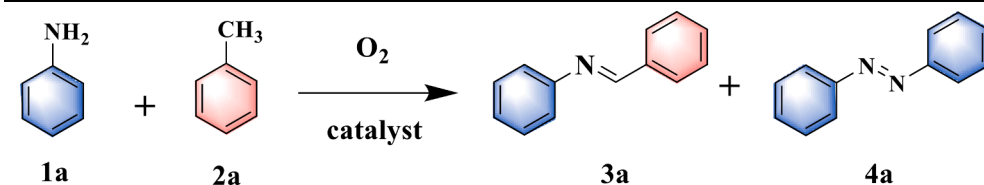


Fig. 4. (a) Co 2p and (b) N1s XPS spectra of Co-N-C/700-0.1 and Co-N-C/800-0.1 catalysts.

Table 1
Catalytic oxidative imination of toluene over different catalysts.^a



Entry	Catalyst	Conversion of 1a (%)	Yield of 3a (%)	Yield of 4a (%)
1	Blank	Trace	Trace	Trace
2	Co-N-C/700-0.1	86	85	<1
3	Co-N-C/800-0.1	>99	98	2
4	Co-N-C/900-0.1	78	77	<1
5	Co-N-C/800-0.2	86	83	3
6	Co-N-C/800-0.1@SiO ₂	60	59	<1
7	Co(NO ₃) ₂ ·6H ₂ O	30	19	11
8	NC	8	8	<1
9	Co-C	45	44	<1

^a Reaction conditions: aniline (0.5 mmol), toluene (3 mL), catalyst (20 mg), O₂ (0.4 MPa), 160 °C, 12 h.

0.20 nm, indicating the presence of the (111) crystal plane belonging to the metallic Co⁰ phase. It is consistent with the results of XRD patterns [42,43]. Furthermore, the elemental mappings of Co-N-C/800-0.1 catalyst (Fig. 3c) revealed that C, O, N and Co elements were well dispersed on the catalyst surface. However, in addition to the above four elements, a small amount of silicon has been detected on the surface of Co-N-C/800-0.1 catalyst, which may be a residue after pickling (Figure S3, Table S2). As seen from the TEM images of Fig. 3d and Figure S4, the agglomeration of Co nanoparticles was severe in Co-C as well as Co-N-C/900-0.1, demonstrating that the doping of N atoms is conducive to the dispersion of Co nanoparticles, but excessive pyrolysis temperatures would result in the agglomeration of the nanoparticles.

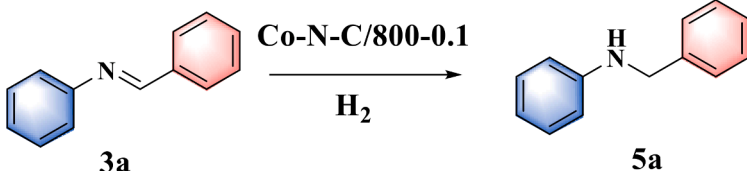
In addition, the surface elemental compositions of Co-N-C catalysts were determined by XPS analysis. The results (Figure S5) verified the presence of Co, O, N and C in the catalysts. To determine the Co species on the surface, high-resolution spectra of Co 2p were analyzed carefully, and the handled results were shown in Fig. 4a. It is indicated that the

binding energies including metallic Co (778.8 eV 2p_{3/2} and 793.8 eV 2p_{1/2}), Co³⁺ (780.7 eV 2p_{3/2} and 795.8 eV 2p_{1/2}) and Co²⁺ (782.8 eV 2p_{3/2} and 797.8 eV 2p_{1/2}), with two satellite peaks at 785.9 eV and 800.7 eV [44,45]. The detection of Co³⁺ and Co²⁺ peaks implies the presence of Co oxides derived from the inevitable metallic Co oxidation on the catalyst surfaces. This phenomenon is commonly found on surfaces of metal-based heterogeneous catalysts. Moreover, Fig. 4b displays the high-resolution N 1s spectra. The deconvoluted peaks of N 1s spectra include four peaks centering at 398.5 eV, 400.2 eV, 401.2 eV, and 403.7 eV, belonging to pyridinic N, pyrrolic N, graphitic N, and oxidized N, respectively [46,47].

3.2. Synthesis of N-benzylaniline

Synthesis of N-benzylaniline involves two steps: (i) the preparation of intermediate benzalaniline; (ii) the preparation of target product N-benzylaniline. The first step was achieved via the oxidative imination of

Table 2
Hydrogenation of benzalaniline to *N*-benzylaniline.^a



Entry	Time (h)	Pressure (MPa)	Conversion of 3a (%)	Yield of 5a (%)
1	6	0.8	55	55
2	9	0.8	85	85
3	12	0.4	16	16
4 ^b	12	0.8	79	79
5 ^c	12	0.8	90	90
6	12	0.8	>99	>99

^a The oxygen in the autoclave was replaced with hydrogen after the first step, and the reaction was performed at 150 °C.

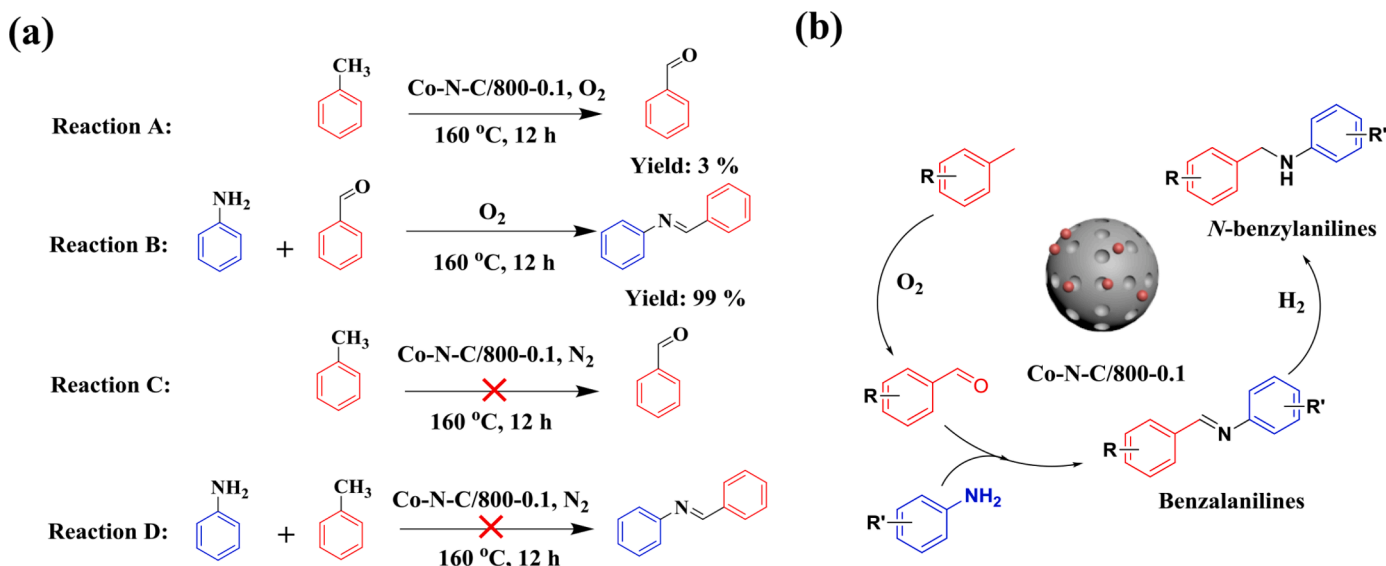
^b The reaction temperature was 130 °C.

^c The reaction temperature was 140 °C.

toluene (Table 1). Initially, a blank-control experiment without catalyst was carried out (Table 1, entry 1), and no product was detected. Then, the catalytic performances of Co-N-C/900-0.1, Co-N-C/700-0.1, and Co-N-C/800-0.1 catalysts were tested (Table 1, entries 2–4). Among them, the Co-N-C/800-0.1 presented the highest catalytic performance, exhibiting the most remarkable performance, with an aniline conversion of 99 % and a benzalaniline yield of 98 % (3a). It was noted that a trace amount of by-product 1, 2-diphenyldiazene (4a) was produced in this process, which was generated by the oxidative coupling of aniline. And the optimized reaction conditions for *N*-benzalaniline synthesis were set as Co-N-C/800-0.1 catalyst (20 mg, 2.3 mol%), 0.4 MPa O₂, 160 °C, and 12 h (Table S3). In contrast, the yields of 3a for Co-N-C/700-0.1 and Co-N-C/900-0.1 were 85 % and 77 %, respectively. Additionally, the yields of 3a for Co-N-C/800-0.2 and Co-N-C/800-0.1@SiO₂ catalysts were 83 % and 59 %, respectively (Table 1, entries 5 and 6). Moreover, the corresponding TOF of these catalysts were calculated, among which Co-N-C/700-0.1 and Co-N-C/800-0.1 catalysts showed relatively good performance (Table S1). These indicate that abundant mesoporous pores and good dispersion of Co nanoparticles are positive to the catalytic activity of Co-N-C catalyst, which corresponds with the results of N₂ adsorption-desorption analysis and TEM characterization. To prove the

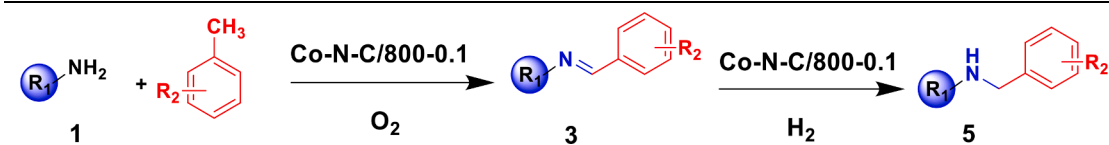
vital role of the Co-N-C/800-0.1 in the reaction, several reference catalysts were carried out under the same experimental conditions. The yield of 3a for Co(NO₃)₂·6H₂O was only 19% (Table 1, entry 7), demonstrating that Co(NO₃)₂·6H₂O cannot effectively catalyze the oxidative imination of toluene. Subsequently, the NC and Co-C catalysts produced 3a in 8 % and 44 % yields (Table 1, entries 8,9), respectively, demonstrating that well-dispersed Co nanoparticles and nitrogen dopant are indispensable for the best performance of catalyst.

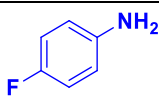
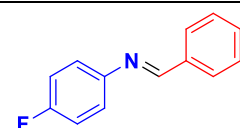
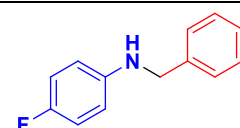
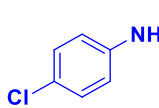
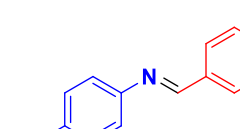
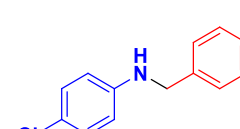
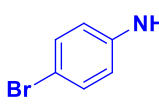
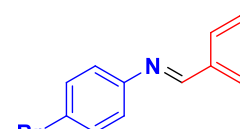
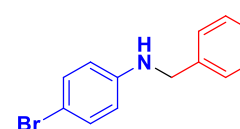
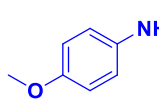
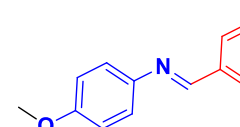
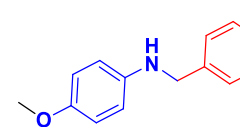
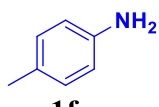
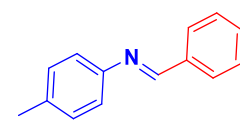
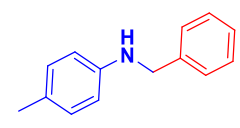
In the first step, the intermediate benzalaniline (3a) was obtained by the oxidative imination of toluene. In the second step, the oxygen atmosphere in the reactor was changed to hydrogen atmosphere for the preparation of target product *N*-benzylaniline (5a). The results are displayed in Table 2. What is gratifying is that benzalaniline (3a) obtained in the first step can be further hydrogenated into *N*-benzylaniline (5a) with high efficiency. After screening the reaction conditions for the hydrogenation of 3a into 5a, the optimized conditions for achieving 99 % yield of 5a were as follows: Co-N-C/800-0.1 catalyst (20 mg, 2.3 mol %), 0.8 MPa H₂, 150 °C, and 12 h.



Scheme 3. (a) Control experiments for the oxidative imination of toluene; (b) Possible reaction pathway for the amination of toluene.

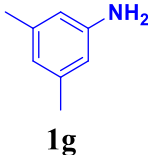
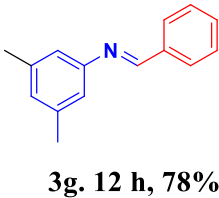
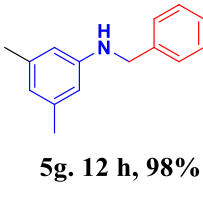
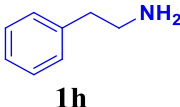
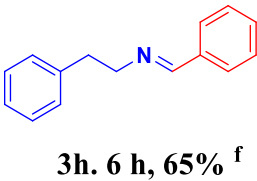
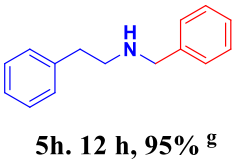
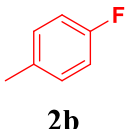
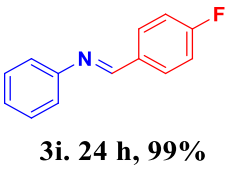
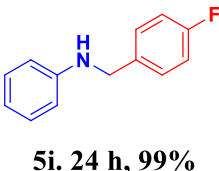
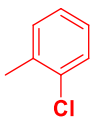
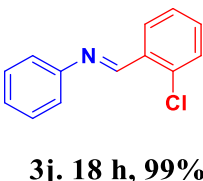
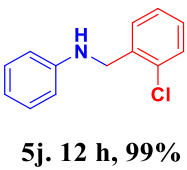
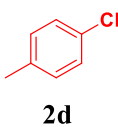
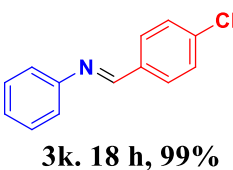
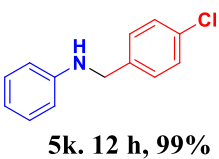
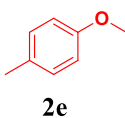
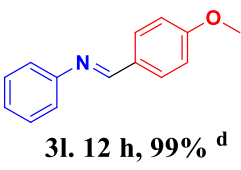
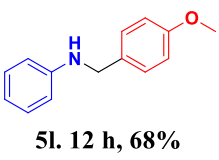
Table 3

Synthesis of various *N*-benzylanilines from toluene derivatives and aniline derivatives over the Co-N-C/800-0.1 catalyst.

Entry	Substrate	Benzalanilines (3) ^a	<i>N</i> -Benzylanilines (5) ^b
1	 1b	 3b. 24 h, 96%^c	 5b. 12 h, 95%
2	 1c	 3c. 18 h, 84%	 5c. 24 h, 94%
3	 1d	 3d. 18 h, 75%	 5d. 24 h, 86%
4	 1e	 3e. 12 h, 75%^d	 5e. 12 h, 78%
5	 1f	 3f. 12 h, 85%	 5f. 12 h, 95%

(continued on next page)

Table 3 (continued)

Entry	Substrate	Benzalanilines (3) ^a	N-Benzylanilines (5) ^b
6		 3g. 12 h, 78%	 5g. 12 h, 98% ^e
7		 3h. 6 h, 65% ^f	 5h. 12 h, 95% ^g
8		 3i. 24 h, 99%	 5i. 24 h, 99%
9		 3j. 18 h, 99%	 5j. 12 h, 99%
10		 3k. 18 h, 99%	 5k. 12 h, 99%
11		 3l. 12 h, 99% ^d	 5l. 12 h, 68%

Reaction conditions:.

^c150 °C;.^d120 °C;.^e170 °C;.

^f100 °C;

^g170 °C.

^a substrate (0.5 mmol), toluene (3 mL), 20 mg catalyst, 160 °C, 12 h, 0.4 MPa O₂;

^b 1.0 MPa H₂.

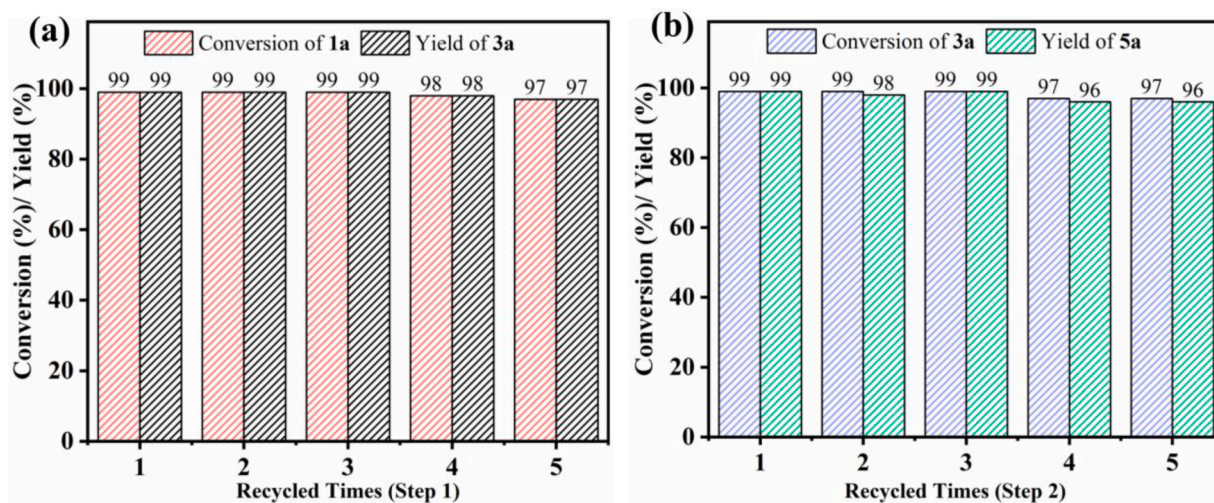


Fig. 5. Assessment of the recyclability of the Co-N-C/800-0.1 catalyst by the measurements of the yields of (a) 3a and (b) 5a.

3.3. Control experiments

Several controlled experiments were performed to investigate the possible reaction pathway for oxidative amination of toluene over Co-N-C/800-0.1 catalyst (Scheme 3a). Under a pure O₂ atmosphere, toluene was converted into benzaldehyde with a yield of 3% (Scheme 3a, Reaction A) with the presence of the Co-N-C/800-0.1 catalyst. Without the addition of catalyst, a condensation reaction between aniline and benzaldehyde produced *N*-benzalaniline with a 99% yield (Scheme 3a, Reaction B), demonstrating that the catalyst is unnecessary in the condensation reaction [48]. Then, two control experiments were conducted under a pure N₂ atmosphere (Scheme 3a, Reactions C and D). The results indicated that toluene could not be converted to benzaldehyde when O₂ was absent, even when aniline was present. On the basis of these results, the possible reaction pathways for amination of toluene were proposed (Scheme 3b). The terminal C(sp³)-H bond of toluene was activated through synergistic catalysis between Co-N-C/800-0.1 catalyst and molecular oxygen, accordingly with the formation of benzaldehyde. Then the obtained benzaldehyde immediately condensed with aniline to form benzalaniline. Finally, the resulting benzalaniline was readily hydrogenated to corresponding *N*-benzylaniline product.

3.4. Applicability and reusability of Co-N-C/800-0.1

Applicability and reusability are essential for examining the performance of a catalyst. The scope of toluene and aniline for this cascade process with Co-N-C/800-0.1 was explored. As shown in Table 3, aniline derivatives with drawing aromatic substituents (-F, -Cl, and -Br) gave the corresponding products in appreciable yields (Table 3, 3b-d). Ether-, methyl- and dimethyl-containing aniline provided the target imines product in 75%, 85% and 78% yields, respectively (Table 3, 3e-g). It seems that the electronic properties of the substituents have a strong influence on the oxidative imination of toluene. When phenethylamine was employed as starting materials, the product 3h was in 65% yield. In addition, toluene derivatives with electron donor or withdrawing groups were also investigated, resulting in the products 3i-3l with high efficiency. To further enlarge the substrate scope, the second step was also investigated by using various aniline derivatives and toluene derivatives as starting materials. With the optimized reaction conditions for this

cascade process in hands, the subsequent hydrogenation process was initiated at the end of the first step process. To our delight, the target secondary amines could be generated with a yield of 68% ~ 99% (Table 3, 5b-l). The identification of the above imines and secondary amines was performed by GC-MS (Figure S6). And the GC-MS full mass spectrums of all the reaction mixtures were shown in Figure S7. Moreover, a hot filtration test was performed to assess the catalyst leaching, as shown in Figure S8. The Co-N-C/800-0.1 catalyst was removed before the reaction was complete. The results revealed that the yield of benzalaniline (3a) did not increase after the Co-N-C/800-0.1 catalyst was filtered, effectively proving that the catalytic process was heterogeneous. Moreover, the Co-N-C/800-0.1 exhibited good stability as well as recycling stability, as there were no significant decreases in the yields of 3a and 5a over five cycles (Fig. 5). Compared with the fresh Co-N-C/800-0.1, XRD patterns of the reused Co-N-C/800-0.1 showed no distinct structure change (Figure S9). Besides, the SEM and energy-dispersive X-ray EDS analysis revealed that there was no significant change in the morphology of catalyst and surface element proportions after five cycles (Figure S10, Table S2). Furthermore, the average size of Co nanoparticles (9.03 ± 0.24 nm) of reused Co-N-C/800-0.1 did not change significantly (Figure S11). Overall, these results highlighted the excellent stability, recyclability, and substrate applicability of Co-N-C/800-0.1.

4. Conclusion

In summary, a highly active cobalt-based catalyst was prepared using a sacrificial template method and applied to a cascade protocol for efficient synthesis of *N*-benzylanilines via oxidative amination of toluene followed by hydrogenation. Under optimal reaction conditions, the target product *N*-benzylaniline could be obtained with a 99% yield. Characterization and control experiments further revealed that the well-dispersed cobalt nanoparticles in catalyst Co-N-C/800-0.1 played a positive role in cascade synthesis of *N*-benzylaniline. In addition, various aromatic amines with 65%–99% yields could be also achieved, showing the excellent applicability and reusability of Co-N-C/800-0.1 catalyst. This work provides a potential avenue for synthesis of aromatic amines using inexpensive and available aromatic alkanes as raw materials.

CRedit authorship contribution statement

Fei-Feng Mao: Investigation, Writing – original draft, Data curation. **Wen-Qiang Gong:** Methodology, Investigation. **Song Han:** Methodology, Investigation. **Yan Zhou:** Methodology, Investigation. **Ming-Shuai Sun:** Writing – review & editing, Methodology, Investigation. **Zhang-Min Li:** Writing – review & editing, Methodology. **Duan-Jian Tao:** Writing – review & editing, Supervision, Resources, Funding acquisition, Conceptualization.

Declaration of competing interest

The authors declare that they have no known competing financial interests or personal relationships that could have appeared to influence the work reported in this paper.

Data availability

Data will be made available on request.

Acknowledgments

We thank the National Natural Science Foundations of China (22378178) and the Key Lab of Fluorine and Silicon for Energy Materials and Chemistry of Ministry of Education, Jiangxi Normal University (KFSEMC-202209) for financial support.

Supplementary materials

Supplementary material associated with this article can be found, in the online version, at [doi:10.1016/j.mcat.2024.113912](https://doi.org/10.1016/j.mcat.2024.113912).

References

- K.I. Goldberg, A.S. Goldman, Large-scale selective functionalization of alkanes, *Acc. Chem. Res.* 50 (3) (2017) 620–626, <https://doi.org/10.1021/acs.accounts.6b00621>.
- X.X. Tang, X.Q. Jia, Z. Huang, Challenges and opportunities for alkane functionalisation using molecular catalysts, *Chem. Sci.* 9 (2) (2018) 288–299, <https://doi.org/10.1039/c7sc03610h>.
- P. Thiruvengadam, D.K. Chand, Controlled and predictably selective oxidation of activated and unactivated C(sp³)–H bonds catalyzed by a molybdenum-based metallomicellar catalyst in water, *J. Org. Chem.* 87 (6) (2022) 4061–4077, <https://doi.org/10.1021/acs.joc.1c02855>.
- Z. Khorsandi, S.F.M. Metkazini, A. Heydari, R.S. Varma, Visible light-driven direct synthesis of ketones from aldehydes via C–H bond activation using NiCu nanoparticles adorned on carbon nano onions, *Mol. Catal.* 516 (2021) 111987, <https://doi.org/10.1016/j.mcat.2021.111987>.
- X. Hu, Y.C. Liu, H.T. Huang, B.B. Huang, G.L. Chai, Z.L. Xie, Template-free synthesis of graphene-like carbons as efficient carbocatalysts for selective oxidation of alkanes, *Green. Chem.* 22 (4) (2020) 1291–1300, <https://doi.org/10.1039/c9gc03781k>.
- D. Zhu, J.Q. Hai, L.Y. Wang, X.L. Long, A study on the oxidation of toluene to benzaldehyde by air catalyzed by polyoxometalate loaded on activated carbon, *Mol. Catal.* 551 (2023) 113626, <https://doi.org/10.1016/j.mcat.2023.113626>.
- W.H. Yang, X.G. Zhao, Y. Wang, X.Y. Wang, H. Liu, W.N. Yang, H. Zhou, Y.A. Wu, C.J. Sun, Y. Peng, J.H. Li, Atomically dispersed ag on δ-MnO₂ cations vacancies trapping for toluene catalytic oxidation, *Catal. Sci. Technol.* 12 (19) (2022) 5932–5941, <https://doi.org/10.1039/d2cy01102f>.
- W.H. Wang, N.Z. Shang, J.M. Wang, X.H. Nie, C.C. Du, X. Zhou, X. Cheng, W. Gao, X. Liu, J.Y. Huang, A stable single-atom Zn catalyst synthesized by a ligand-stabilized pyrolysis strategy for selective oxidation of C–H bonds, *Green. Chem.* 24 (15) (2022) 6008–6015, <https://doi.org/10.1039/d2gc01831d>.
- S. Mehrabi-Kalajahi, Y. Orooji, S. Arefi Oskoui, M.A. Varfolomeev, N. M. Khasanova, Y. Yoon, A. Khataee, Preparation of layered V₄AIC₃ max phase for highly selective and efficient solvent-free aerobic oxidation of toluene to benzaldehyde, *Mol. Catal.* 529 (2022) 112545, <https://doi.org/10.1016/j.mcat.2022.112545>.
- H. Yi, G.T. Zhang, H.M. Wang, Z.Y. Huang, J. Wang, A.K. Singh, A.W. Lei, Recent advances in radical C–H activation/radical cross-coupling, *Chem. Rev.* 117 (13) (2017) 9016–9085, <https://doi.org/10.1021/acs.chemrev.6b00620>.
- S.K. Kariofillis, A.G. Doyle, Synthetic and mechanistic implications of chlorine photoelimination in nickel/photoredox C(sp³)–H cross-coupling, *Acc. Chem. Res.* 54 (4) (2021) 988–1000, <https://doi.org/10.1021/acs.accounts.0c00694>.
- J.R. Clark, K.B. Feng, A. Sookezian, M.C. White, Manganese-catalysed benzylic C(sp³)–H amination for late-stage functionalization, *Nat. Chem.* 10 (6) (2018) 583–591, <https://doi.org/10.1038/s41557-018-0020-0>.
- B. Liu, A.M. Romine, C.Z. Rubel, K.M. Engle, B.F. Shi, Transition-metal-catalyzed, coordination-assisted functionalization of nonactivated C(sp³)–H bonds, *Chem. Rev.* 121 (24) (2021) 14957–15074, <https://doi.org/10.1021/acs.chemrev.1c00519>.
- A. Trowbridge, S.M. Walton, M.J. Gaunt, New strategies for the transition-metal catalyzed synthesis of aliphatic amines, *Chem. Rev.* 120 (5) (2020) 2613–2692, <https://doi.org/10.1021/acs.chemrev.9b00462>.
- K. Murugesan, T. Senthamarai, V.G. Chandrashekhar, K. Natte, P.C.J. Kamer, M. Beller, R.V. Jagadeesh, Catalytic reductive aminations using molecular hydrogen for synthesis of different kinds of amines, *Chem. Soc. Rev.* 49 (17) (2020) 6273–6328, <https://doi.org/10.1039/c9cs00286c>.
- Z. Ma, B. Zhou, X.M. Li, R.G. Kadam, M.B. Gawande, M. Petr, R. Zboril, M. Beller, R.V. Jagadeesh, Reusable Co-nanoparticles for general and selective n-alkylation of amines and ammonia with alcohols, *Chem. Sci.* 13 (1) (2022) 111–117, <https://doi.org/10.1039/d1sc05913k>.
- Y.Z. Xu, Y.R. Liu, P.L. Cui, N.Z. Shang, C. Wang, Y.J. Gao, Stable Ni catalyst encapsulated in N-doped carbon nanotubes for one-pot reductive amination of nitroarenes with aldehydes, *Appl. Catal. A, Gen.* 622 (2021) 118230, <https://doi.org/10.1016/j.apcata.2021.118230>.
- H. Yao, B. Xie, X.Y. Zhong, S.Z. Jin, S. Lin, Z.H. Yan, Copper-catalyzed direct amination of benzylic hydrocarbons and inactive aliphatic alkanes with arylamines, *Org. Biomol. Chem.* 18 (17) (2020) 3263–3268, <https://doi.org/10.1039/d0ob00491j>.
- Y.L. Song, B. Li, Z.B. Xie, D. Wang, H.M. Sun, Iron-catalyzed oxidative amination of benzylic C(sp³)–H bonds with anilines, *J. Org. Chem.* 86 (24) (2021) 17975–17985, <https://doi.org/10.1021/acs.joc.1c02311>.
- A. Brandt, A.B. RanguMagar, P. Szewdo, H.A. Wayland, C.M. Parnell, P. Munshi, A. Ghosh, Highly economical and direct amination of sp³ carbon using low-cost nickel pincer catalyst, *RSC. Adv.* 11 (3) (2021) 1862–1874, <https://doi.org/10.1039/d0ra09639c>.
- S.F. Pang, F. Shi, Oxidative amination of benzylic alkanes with nitrobenzene derivatives as nitrogen sources, *Tetrahedron. Lett.* 57 (52) (2016) 5872–5876, <https://doi.org/10.1016/j.tetlet.2016.11.057>.
- A.M. Voutchkova, R.H. Crabtree, Iridium-catalyzed benzylic C–H activation and functionalization of alkyl arenes, *J. Mol. Catal. A: Chem.* 312 (1–2) (2009) 1–6, <https://doi.org/10.1016/j.molcata.2009.07.019>.
- X.Y. Yu, L.J. Wang, X. Wang, H.Z. Liu, Z.Y. Wang, Y.X. Huang, G.Q. Shan, W. C. Wang, L.Y. Zhu, Enhanced nonradical catalytic oxidation by encapsulating cobalt into nitrogen doped graphene: highlight on interfacial interactions, *J. Mater. Chem. A* 9 (11) (2021) 7198–7207, <https://doi.org/10.1039/d0ta10662c>.
- Y.S. Liu, Z.C. Chen, N. Zhao, G.C. Tong, Z.X. Li, B.Q. Wang, Y. Du, Q.Y. Pan, Z. Li, Y.L. Xie, Ultra-small cobalt nanoparticles embedded into N-doped hierarchical porous carbon derived from ion-exchange MOFs as high-efficient bifunctional catalysts for rechargeable Zn-air battery, *Chem. Eng. J.* 433 (2022) 134469, <https://doi.org/10.1016/j.cej.2021.134469>.
- Y.X. Gong, N. Wang, E.Y. Gao, Q.Q. Wan, X. Bai, X.Y. He, B. Zhao, Y.Q. Zhang, H. B. Yu, Q. Liu, P. Liang, B. Xu, G.M. Zhao, X. Fan, Nitrogen-doped carbon confined cobalt nanoparticles as the steric acid-base multifunctional catalysts for knoevenagel condensation, *Mol. Catal.* 550 (2023) 113521, <https://doi.org/10.1016/j.mcat.2023.113521>.
- Z. Khorsandi, A.R. Hajipour, M.R. Sarfjoo, R.S. Varma, Cobalt nanoparticle adorned on boron- and nitrogen-doped 2d-carbon material for sonogashira cross-coupling reactions: greener and efficient synthesis of anti-cancer drug, ponatinib, *Mol. Catal.* 532 (2022) 112701, <https://doi.org/10.1016/j.mcat.2022.112701>.
- D. Li, W.H. Chen, J.P. Wu, C.Q. Jia, X. Jiang, The preparation of waste biomass-derived N-doped carbons and their application in acid gas removal: focus on N functional groups, *J. Mater. Chem. A* 8 (47) (2020) 24977–24995, <https://doi.org/10.1039/d0ta07977d>.
- S. Han, R.J. Gao, M.S. Sun, Y. Zhou, W.T. Chen, X.X. Liu, J.Z. Qin, D.J. Tao, Synergistic roles of single Co atoms and Co nanoparticles for the hydrodeoxygenation and ring hydrogenation reactions, *J. Phys. Chem. C* 127 (29) (2023) 14185–14196, <https://doi.org/10.1021/acs.jpcc.3c02352>.
- S. Nandi, P. Patel, N.U.H. Khan, A.V. Biradar, R.I. Kureshy, Nitrogen-rich graphitic-carbon stabilized cobalt nanoparticles for chemoselective hydrogenation of nitroarenes at milder conditions, *Inorg. Chem. Front.* 5 (4) (2018) 806–813, <https://doi.org/10.1039/c7qi00772h>.
- S. Han, W.T. Chen, Z.T. Gao, H. Guan, Z.M. Li, D.J. Tao, Mechanochemical-assisted synthesis of nitrogen-doped carbon supported cobalt catalysts for efficient and selective hydrogenation of furfural, *Catal. Lett.* 153 (4) (2022) 956–964, <https://doi.org/10.1007/s10562-022-04042-y>.
- B. Zeng, L. Chen, G.L. Zhu, B.X. Yang, C.G. Xia, L. He, Nitrogen-doped cobalt nanocatalysts for carbonylation of propylene oxide, *Mol. Catal.* 494 (2020) 111109, <https://doi.org/10.1016/j.mcat.2020.111109>.
- H.A. Khan, P. Natarajan, K.D. Jung, Stabilization of Pt at the inner wall of hollow spherical SiO₂ generated from Pt/hollow spherical SiC for sulfuric acid decomposition, *Appl. Catal. B: Environ.* 231 (2018) 151–160, <https://doi.org/10.1016/j.apcatb.2018.03.013>.
- Z.H. Meng, N. Chen, S.C. Cai, R. Wang, W.B. Guo, H.L. Tang, Co-N-doped hierarchically ordered macro/mesoporous carbon as bifunctional electrocatalyst toward oxygen reduction/evolution reactions, *Int. J. Energy Res.* 45 (4) (2020) 6250–6261, <https://doi.org/10.1002/er.6247>.
- S. Seo, W. Chaikittisilp, N. Koike, T. Yokoi, T. Okubo, Porous inorganic-organic hybrid polymers derived from cyclic siloxane building blocks: effects of

- substituting groups on mesoporous structures, *Microporous Mesoporous Mater.* 278 (2019) 212–218, <https://doi.org/10.1016/j.micromeso.2018.11.016>.
- [35] W.H. Tang, K.W. Teng, W.G. Guo, F. Gu, B.Y. Li, R.Y. Qi, R.P. Liu, Y.Y. Lin, M. M. Wu, Y.H. Chen, Defect-engineered Co_3O_4 @nitrogen-deficient graphitic carbon nitride as an efficient bifunctional electrocatalyst for high-performance metal-air batteries, *Small*. 18 (27) (2022) 2202194, <https://doi.org/10.1002/smll.202202194>.
- [36] H. Torabi, H. Eshghi, S.S.E. Ghodsinia, P. Sanati-Tirgan, Design and synthesis of ZnGlu MOF/SBA-16 nanocomposite, and its performance as an environmentally friendly nanocomposite for solvent-free chemical fixation of CO_2 to epoxides for high-yield synthesis of cyclic carbonates, *Mol. Catal.* 550 (2023) 113552, <https://doi.org/10.1016/j.mcat.2023.113552>.
- [37] X.M. Lu, J.Z. Qin, C.S. Xian, J.B. Nie, X. Li, J. He, B. Liu, Cobalt nanoparticles supported on microporous nitrogen-doped carbon for an efficient catalytic transfer hydrogenation reaction between nitroarenes and n-heterocycles, *Catal. Sci. Technol.* 12 (18) (2022) 5549–5558, <https://doi.org/10.1039/d2cy00914e>.
- [38] K. Li, Y.Z. Wu, M.P. Chen, Q. Rong, Z.Q. Zhu, Q.J. Liu, J. Zhang, High methanol gas-sensing performance of $\text{Sm}_2\text{O}_3/\text{ZnO}/\text{SmFeO}_3$ microspheres synthesized via a hydrothermal method, *Nanoscale Res. Lett.* 14 (1) (2019) 57, <https://doi.org/10.1186/s11671-019-2890-5>.
- [39] C.H. Zhang, Y.L. Guo, Y. Guo, G.Z. Lu, A. Boreave, L. Retailleau, A. Baylet, A. Giroir-Fendler, LaMnO_3 perovskite oxides prepared by different methods for catalytic oxidation of toluene, *Appl. Catal. B* 148–149 (2014) 490–498, <https://doi.org/10.1016/j.apcatb.2013.11.030>.
- [40] S.B. Zou, M.Y. Zhang, S.P. Mo, H.R. Cheng, M.L. Fu, P.R. Chen, L.M. Chen, W. Shi, D.Q. Ye, Catalytic performance of toluene combustion over Pt nanoparticles supported on pore-modified macro-meso-microporous zeolite foam, *Nanomaterials* 10 (1) (2019) 30, <https://doi.org/10.3390/nano10010030>.
- [41] P. Zhou, L. Jiang, F. Wang, K.J. Deng, K. Lv, Z.H. Zhang, High performance of a cobalt–nitrogen complex for the reduction and reductive coupling of nitro compounds into amines and their derivatives, *Sci. Adv.* 3 (2) (2017) e1601945, <https://doi.org/10.1126/sciadv.1601945>.
- [42] Y.Y. Xue, Y.B. Guo, Q.M. Zhang, Z.J. Xie, J.P. Wei, Z. Zhou, MOF-derived Co and Fe species loaded on N-doped carbon networks as efficient oxygen electrocatalysts for Zn-air batteries, *Nano-Micro Lett.* 14 (1) (2022) 162, <https://doi.org/10.1007/s40820-022-00890-w>.
- [43] H. Yang, S. Gao, D.W. Rao, X.H. Yan, Designing superior bifunctional electrocatalyst with high-purity pyrrole-type CoN_4 and adjacent metallic cobalt sites for rechargeable Zn-air batteries, *Energy Storage Mater.* 46 (2022) 553–562, <https://doi.org/10.1016/j.ensm.2022.01.040>.
- [44] J. Yu, G. Chen, J. Sunarso, Y.L. Zhu, R. Ran, Z.H. Zhu, W. Zhou, Z.P. Shao, Cobalt oxide and cobalt-graphitic carbon core-shell based catalysts with remarkably high oxygen reduction reaction activity, *Adv. Sci.* 3 (9) (2016) 1600060, <https://doi.org/10.1002/advs.201600060>.
- [45] O.Y. Bisen, R. Nandan, A.K. Yadav, B. Pavithra, K.Kar Nanda, In situ self-organization of uniformly dispersed Co–N–C centers at moderate temperature without a sacrificial subsidiary metal, *Green. Chem.* 23 (8) (2021) 3115–3126, <https://doi.org/10.1039/d0gc04050a>.
- [46] J.Q. Jiao, N.N. Zhang, C. Zhang, N. Sun, Y. Pan, C. Chen, J. Li, M.J. Tan, R.X. Cui, Z.L. Shi, J.W. Zhang, H. Xiao, T.B. Lu, Doping ruthenium into metal matrix for promoted pH-universal hydrogen evolution, *Adv. Sci.* 9 (15) (2022) 2200010, <https://doi.org/10.1002/advs.202200010>.
- [47] S.C. Wu, M. Zhao, Z.J. Xia, J.H. Liu, Y.Q. Chen, Z.L. Xie, Nitrogen incorporation endows copper notable activity for the selective reduction of nitroarenes, *Mol. Catal.* 550 (2023) 113583, <https://doi.org/10.1016/j.mcat.2023.113583>.
- [48] X.Y. Zhang, J.H. Zhang, Z.Q. Hao, Z.G. Han, J. Lin, G.L. Lu, Nickel complexes bearing N, N, O-tridentate salicylaldiminato ligand: efficient catalysts for imines formation via dehydrogenative coupling of primary alcohols with amines, *Organometallics* 40 (22) (2021) 3843–3853, <https://doi.org/10.1021/acs.organomet.1c00552>.